A UNIFIED APPROACH TO JOINT REGIONAL/TELESEISMIC CALIBRATION AND EVENT LOCATION WITH A 3D EARTH MODEL

William L. Rodi[1], Delaine T. Reiter[2], Stephen C. Myers[3], and Nathan A. Simmons[3]

Massachusetts Institute of Technology[1], Weston Geophysical Corporation[2], and Lawrence Livermore National Laboratory[3]

Sponsored by the National Nuclear Security Administration

Award Nos. DE-AC52-08NA28539[1, 2] and DE-AC52-07NA27344[3]
Proposal No. BAA08-19

ABSTRACT

This project investigates the problem of locating seismic events from combined data sets of regional and teleseismic arrival times, based on the use of a unified 3D model of the Earth's velocity structure to predict travel times for both types of data. Inherent to this problem is the joint tomographic calibration of the Earth model with both regional and teleseismic ground-truth data. The goal of the unified approach is to remove the inconsistencies that result when travel-time predictions are performed with a mixture of separately calibrated regional and global models and empirical corrections, which can lead to degradation of event location performance. Numerical experiments we have performed with joint regional/teleseismic travel-time tomography have demonstrated, for example, that joint calibration preempts a baseline shift between regional and teleseismic travel-time predictions.

Our project has focused largely on the practical difficulties of implementing a unified location/calibration capability. One such difficulty is the computational challenge of performing tomographic inversion with very large numbers of data and model parameters. Available data bases, for example, contain many millions of regional and teleseismic arrivals while 3D Earth models with appropriate resolution contain millions of grid nodes. Travel-time computation in 3D models presents another significant challenge. It can require days of central processing unit (CPU) time to forward model a travel-time data set when a fully 3D raytracing methods is used.

An efficient alternative to full 3D raytracing is travel-time linearization, which approximates the travel time in a 3D model by integrating its slowness function along the raypath computed in a 1D reference model. Our numerical experiments with this approach have shown that it is quite accurate for teleseismic travel times, as judged by comparing to travel times calculated with a highly accurate raybending method. While we previously had dismissed linearization as being inadequate for calculating travel times at regional distances, we have recently pursued a modification of the linearization technique that shows promise at least for distances up to ten degrees. The modification involves warping of the Mohorovičić (Moho) discontinuity and other velocity interfaces in the 3D model to match their flat counterparts in the 1D reference model. This paper explains the warping technique and presents some examples showing its promise for modeling regional travel times. We also present preliminary results of joint regional/teleseismic tomography based on the new linearization method.

Report Documentation Page		*Form Approved* *OMB No. 0704-0188*
Public reporting burden for the collection of information is estimated to average 1 hour per response, including the time for reviewing instructions, searching existing data sources, gathering and maintaining the data needed, and completing and reviewing the collection of information. Send comments regarding this burden estimate or any other aspect of this collection of information, including suggestions for reducing this burden, to Washington Headquarters Services, Directorate for Information Operations and Reports, 1215 Jefferson Davis Highway, Suite 1204, Arlington VA 22202-4302. Respondents should be aware that notwithstanding any other provision of law, no person shall be subject to a penalty for failing to comply with a collection of information if it does not display a currently valid OMB control number.		
1. REPORT DATE **SEP 2011**	2. REPORT TYPE	3. DATES COVERED **00-00-2011 to 00-00-2011**
4. TITLE AND SUBTITLE **A Unified Approach to Joint Regional/Teleseismic Calibration and Event Location with a 3D Earth Model**		5a. CONTRACT NUMBER
		5b. GRANT NUMBER
		5c. PROGRAM ELEMENT NUMBER
6. AUTHOR(S)		5d. PROJECT NUMBER
		5e. TASK NUMBER
		5f. WORK UNIT NUMBER
7. PERFORMING ORGANIZATION NAME(S) AND ADDRESS(ES) **Massachusetts Institute of Technology,77 Massachusetts Avenue,Cambridge,MA,02139**		8. PERFORMING ORGANIZATION REPORT NUMBER
9. SPONSORING/MONITORING AGENCY NAME(S) AND ADDRESS(ES)		10. SPONSOR/MONITOR’S ACRONYM(S)
		11. SPONSOR/MONITOR’S REPORT NUMBER(S)
12. DISTRIBUTION/AVAILABILITY STATEMENT **Approved for public release; distribution unlimited**		
13. SUPPLEMENTARY NOTES **Published in the Proceedings of the 2011 Monitoring Research Review - Ground-Based Nuclear Explosion Monitoring Technologies, 13-15 September 2011, Tucson, AZ. Volume I. Sponsored by the Air Force Research Laboratory (AFRL) and the National Nuclear Security Administration (NNSA). U.S. Government or Federal Rights License**		

14. ABSTRACT

This project investigates the problem of locating seismic events from combined data sets of regional and teleseismic arrival times, based on the use of a unified 3D model of the Earth's velocity structure to predict travel times for both types of data. Inherent to this problem is the joint tomographic calibration of the Earth model with both regional and teleseismic ground-truth data. The goal of the unified approach is to remove the inconsistencies that result when travel-time predictions are performed with a mixture of separately calibrated regional and global models and empirical corrections, which can lead to degradation of event location performance. Numerical experiments we have performed with joint regional/teleseismic travel-time tomography have demonstrated, for example, that joint calibration preempts a baseline shift between regional and teleseismic travel-time predictions. Our project has focused largely on the practical difficulties of implementing a unified location/calibration capability. One such difficulty is the computational challenge of performing tomographic inversion with very large numbers of data and model parameters. Available data bases, for example, contain many millions of regional and teleseismic arrivals while 3D Earth models with appropriate resolution contain millions of grid nodes. Travel-time computation in 3D models presents another significant challenge. It can require days of central processing unit (CPU) time to forward model a travel-time data set when a fully 3D raytracing methods is used. An efficient alternative to full 3D raytracing is travel-time linearization, which approximates the travel time in a 3D model by integrating its slowness function along the raypath computed in a 1D reference model. Our numerical experiments with this approach have shown that it is quite accurate for teleseismic travel times, as judged by comparing to travel times calculated with a highly accurate raybending method. While we previously had dismissed linearization as being inadequate for calculating travel times at regional distances, we have recently pursued a modification of the linearization technique that shows promise at least for distances up to ten degrees. The modification involves warping of the Mohorovičić (Moho) discontinuity and other velocity interfaces in the 3D model to match their flat counterparts in the 1D reference model. This paper explains the warping technique and presents some examples showing its promise for modeling regional travel times. We also present preliminary results of joint regional/teleseismic tomography based on the new linearization method.

15. SUBJECT TERMS

16. SECURITY CLASSIFICATION OF:			17. LIMITATION OF ABSTRACT	18. NUMBER OF PAGES	19a. NAME OF RESPONSIBLE PERSON
a. REPORT **unclassified**	b. ABSTRACT **unclassified**	c. THIS PAGE **unclassified**	**Same as Report (SAR)**	**10**	

Standard Form 298 (Rev. 8-98)
Prescribed by ANSI Std Z39-18

OBJECTIVE

Several studies have shown that 3D models of crust and upper mantle velocity structure predict significantly more accurate travel times for regional seismic phases than do 1D global models, leading to more accurate locations for small, regionally recorded events (e.g. Ryaboy et al., 2001; Reiter et al., 2005; Murphy et al., 2005; Flanagan et al., 2007). However, it is not uncommon to also observe teleseismic arrivals from small events of monitoring interest, at least in part of the teleseismic distance range. While adding teleseismic to regional data should in theory improve event locations even further, it has not always been the case in practice. For example, Yang et al. (2004) found that event locations obtained by combining regional and teleseismic data were only more accurate than locations found from the separate data sets if they corrected for a bias between teleseismic and regional travel-time predictions, each made from a different 3D model: CUB1.0 (Ritzwoller et al., 2002) for regional, and J362D28 (Antolik et al., 2003) for teleseismic. The correction they inferred is small (0.79 s) but even small, systematic shifts in teleseismic travel times can induce large location errors owing to the high apparent velocity of teleseismic arrivals.

We are investigating a methodology for seismic event location based on the principle that travel times for all seismic phases should be predicted consistently with a single 3D Earth model. This unified modeling approach would be applied in locating events from combined sets of regional and teleseismic data, and in a joint tomographic inversion to calibrate the 3D model. The feasibility and value of the unified 3D modeling approach has been demonstrated recently by Myers et al. (2011) and Simmons et al. (2011) in companion papers. Our efforts in this project have focused on developing computational methods that improve the efficiency and practicality of joint regional/teleseismic location and calibration.

RESEARCH ACCOMPLISHED

Our project is focusing on the development of a prototype capability for event location and travel-time calibration with 3D Earth models, applicable to regional and teleseismic data. Our goal is not to develop a complete and operations-ready 3D capability, but rather to demonstrate the value and practicality of the unified approach. The following sections describe our progress to date in developing two key components of the approach: 3D travel-time calculation and joint regional/teleseismic tomography.

Travel-Time Linearization

A number of numerical methods are available for raytracing and travel-time calculation in 3D Earth models, such as the finite-difference eikonal method (e.g., Podvin and Lecomte, 1991), fast marching (Rawlinson and Sambridge, 2004), and two-point raybending (e.g., Um and Thurber, 1987). Given the computational intensity of these full 3D methods, many applications, such as global tomography with teleseismic data, have used approximate travel times calculated with linearization around a 1D reference model. We will describe this approach as it is conventionally applied and then propose a modification of the approach that attempts to improve its accuracy.

Let $\mathbf{r}$ denote the position vector in some coordinate system (e.g., with origin at the Earth's center), and consider the travel time, T, between a source point, $\mathbf{r}_1$, and receiver point, $\mathbf{r}_2$, through a 3D velocity function, $v(\mathbf{r})$. Geometrical ray theory implies that T is obtained by integrating the slowness function, $1/v(\mathbf{r})$, along the geometrical ray connecting $\mathbf{r}_1$ and $\mathbf{r}_2$. Denoting the geometric ray as $\bar{\mathbf{r}}$, we can express this as

$$T = \int_{\mathbf{r}_1}^{\mathbf{r}_2} \frac{1}{v(\bar{\mathbf{r}})} |d\bar{\mathbf{r}}|, \tag{1}$$

where $|d\bar{\mathbf{r}}|$ denotes the differential distance along the ray. Fermat's Principle states that T is stationary with respect to perturbations to the ray path, allowing us to approximate the travel time as

$$T \approx \int_{\mathbf{r}_1}^{\mathbf{r}_2} \frac{1}{v(\tilde{\mathbf{r}})} |d\tilde{\mathbf{r}}|, \tag{2}$$

where $\tilde{\mathbf{r}}$ is an approximate ray connecting $\mathbf{r}_1$ and $\mathbf{r}_2$. The accuracy of the approximation is determined by the proximity of $\tilde{\mathbf{r}}$ to $\bar{\mathbf{r}}$.

The standard approach to travel-time linearization applies Equation 2 with $\tilde{\mathbf{r}}$ taken as the geometrical ray in a reference velocity function, v_{ref}. Denoting this ray as $\bar{\mathbf{r}}_{\mathrm{ref}}$, Equation 2 becomes

$$T \approx \int_{\mathbf{r}_1}^{\mathbf{r}_2} \frac{1}{v(\bar{\mathbf{r}}_{\mathrm{ref}})} |d\bar{\mathbf{r}}_{\mathrm{ref}}|. \tag{3}$$

The approximation becomes advantageous when v_{ref} is chosen such that the computation of $\bar{\mathbf{r}}_{\mathrm{ref}}$ is more efficient than the computation of $\bar{\mathbf{r}}$, e.g. when v_{ref} is a 1D velocity model.

Example

In the previous year of the project we conducted numerical experiments to test the accuracy of travel-time linearization for computing travel times in an early version of Lawrence Livermore National Laboratory's (LLNL) 3D Earth model, LLNL-G3D (Simmons et al., 2009). The experiments considered travel times between four station locations and a 3D grid of event locations. The event grid covered the box 15°–55°N, 30°–80°E (roughly, the Middle East) at 1° spacing and contained five event depths between the surface and 120 km. The four stations, each at zero depth, were located at the corners of the event grid. Travel times for the resulting 41,820 event-station paths were calculated with the standard linearization method using the AK135 1D model (Kennett et al., 1995) as the reference model. These times were compared to highly accurate raybending calculations through LLNL-G3D performed with the algorithm described by Simmons et al. (2009).

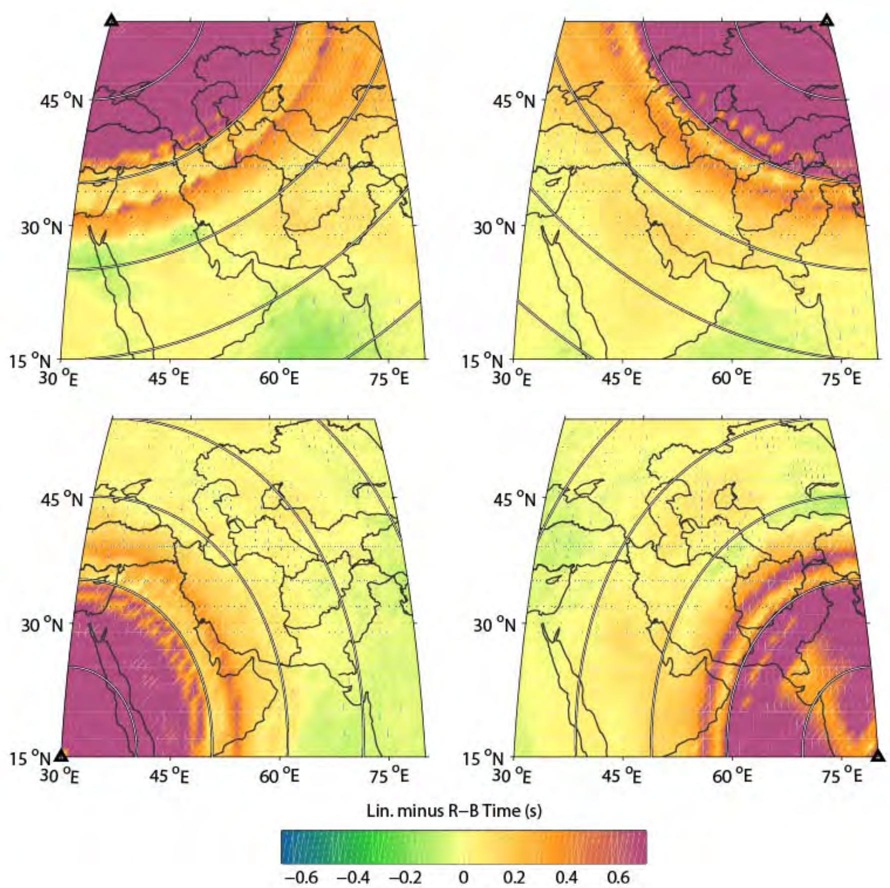

Figure 1. Discrepancy between travel times calculated through model LLNL-G3D with two methods: raybending and linearization. Linearized times were calculated with AK135 as the reference model. Each panel shows the discrepancies for paths connecting a geographic grid of events at 15-km depth to one of four surface stations at the corners of the event grid. The travel-time scale has been clipped at ±0.7 s.

Some results of these tests (also shown in Rodi et al., 2010) are shown in Figures 1 and 2. The figures display the discrepancy between linearized and raybending times, which can be interpreted as the error in the linearization calculations given the high accuracy of the raybending method. Figure 1 plots the travel-time discrepancies as a function of event epicenter, for the events at 15-km depth and for each of the four corner stations (labeled NW, NE, etc.). Figure 2 displays the same results as a histogram binned by travel-time discrepancy and epicentral distance. These results, and those for the other event depths, indicate that the errors in linearized times at teleseismic distances are generally well below 0.5 s. At regional distances, however, the errors can be several seconds or more (up to 30 s for some paths). A major contributor to the large errors at regional distances is the wide variability of Moho depth in Eurasia, from about 10 km under the Indian Ocean to 75 km beneath the Himalayan Mountains. Thus, for example, some first-arriving Pn rays in LLNL-G3D may be contained in the AK135 crust.

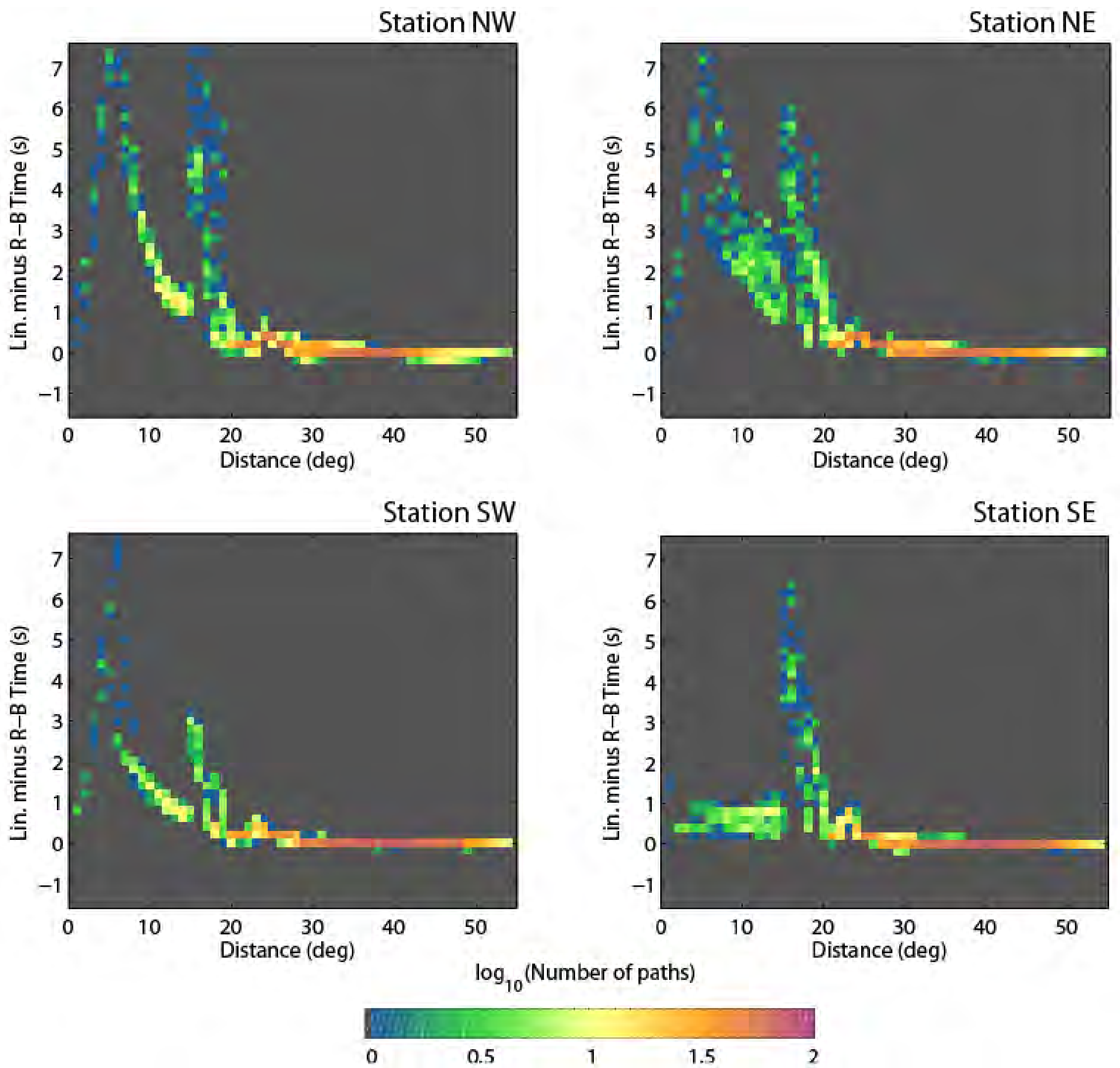

Figure 2. Discrepancy between travel times calculated through model LLNL-G3D with two methods: raybending and linearization. The travel-time discrepancies shown are the same as in Figure 1, but displayed as histograms binned with respect to time discrepancy (with 0.2 s increment) and epicentral distance (1° increment). The time axis is clipped at 7.5 s.

Linearization with Ray Warping

The modification of the linearization method we are investigating attempts to find a better approximation to the geometrical ray, $\bar{\mathbf{r}}$, in the 3D velocity model, $v(\mathbf{r})$. It assumes the approximate ray has the form

$$\tilde{\mathbf{r}} = W(\bar{\mathbf{r}}'_{\mathrm{ref}}), \tag{4}$$

where W is a specified *warping* transformation. The ray $\bar{\mathbf{r}}'_{\mathrm{ref}}$, like $\bar{\mathbf{r}}_{\mathrm{ref}}$, is calculated in v_{ref} but its endpoints are modified by the warping transformation to be

$$\mathbf{r}'_1 = W^{-1}(\mathbf{r}_1) \tag{5}$$
$$\mathbf{r}'_2 = W^{-1}(\mathbf{r}_2), \tag{6}$$

where W^{-1} is the inverse transformation of W. This ensures that $\tilde{\mathbf{r}}$ has the correct endpoints, $\mathbf{r}_1$ and $\mathbf{r}_2$. Substituting Equation 4 into Equation 2 yields

$$T \approx \int_{\mathbf{r}_1}^{\mathbf{r}_2} \frac{1}{v(W(\bar{\mathbf{r}}'_{\mathrm{ref}}))} |dW(\bar{\mathbf{r}}'_{\mathrm{ref}})|. \tag{7}$$

This integration along the warped reference ray can be converted to integration along the reference ray itself with a change of variable. Define the quantity γ at each point of a geometrical ray $\bar{\mathbf{r}}$ as

$$\gamma(\bar{\mathbf{r}}) = \frac{|dW(\bar{\mathbf{r}})|}{|d\bar{\mathbf{r}}|}. \tag{8}$$

The quantity γ is the ratio between the differential distance along the ray before and after warping; it is determined by the local direction of the ray and the Jacobian of W. The conversion of Equation 7 to an integral along the unwarped reference ray then becomes

$$T \approx \int_{\mathbf{r}'_1}^{\mathbf{r}'_2} \frac{\gamma(\bar{\mathbf{r}}'_{\mathrm{ref}})}{v(W(\bar{\mathbf{r}}'_{\mathrm{ref}}))} |d\bar{\mathbf{r}}'_{\mathrm{ref}}|. \tag{9}$$

The objective in this approach is to choose W so that it transforms the reference ray into a better approximation of the geometrical ray in the 3D model. This is consistent with, if not equivalent to, transforming the reference model into a better approximation of the 3D model, i.e., making $v_{\mathrm{ref}}\,(W^{-1}(\mathbf{r}))$ resemble $v(\mathbf{r})$ more closely than $v_{\mathrm{ref}}(\mathbf{r})$ does. Our initial experiments with the approach have attempted to achieve this by choosing W to move points vertically in such a way that the velocity discontinuities of the reference model and 3D model coincide. Then, for example, $W(\bar{\mathbf{r}}'_{\mathrm{ref}})$ will be at the Moho discontinuity of the 3D model when $\bar{\mathbf{r}}'_{\mathrm{ref}}$ is at the Moho of the reference model, ensuring that a Pn ray in the reference model traverses the upper mantle of the 3D model.

Example

To test whether ray warping improves the accuracy of linearized travel-time calculations, we repeated the numerical tests with model LLNL-G3D, described above, replacing the standard linearization method with the new approach. We defined the warping transformation so that the depths of all interfaces in the 1D reference model matched those of LLNL-G3D, which include the ocean bottom; interfaces between as many as three sedimentary layers and three deeper hard-rock crustal layers; and two mantle discontinuities (at 410 and 660 km in AK135). This required adding thin (1-meter) water and sedimentary layers to the AK135 profile to make the reference model compatible with LLNL-G3D.

Figure 3 shows the travel-time discrepancies between linearized travel-time calculations, performed with ray warping, and raybending calculations. The figure displays the discrepancies as distance-dependent histograms and is analogous to Figure 2. Comparing Figures 2 and 3, we can see that ray warping greatly reduces the errors in linearized times at regional distances, up to about 10 degrees of so. The errors at teleseismic distance, however, are increased slightly. Ray warping does not reduce the errors at epicentral distances between about 14° and 24° to acceptable levels. This distance range corresponds to AK135 rays that turn in or near the transition zone.

Figure 4 shows the results of additional accuracy tests involving events at four other depths. The discrepancies in these cases are also much smaller at regional distances than with standard linearization, although some problems occur for surface events (which include events at the top of the ocean), and the deepest events, whose rays are affected by the transition zone at shorter distances.

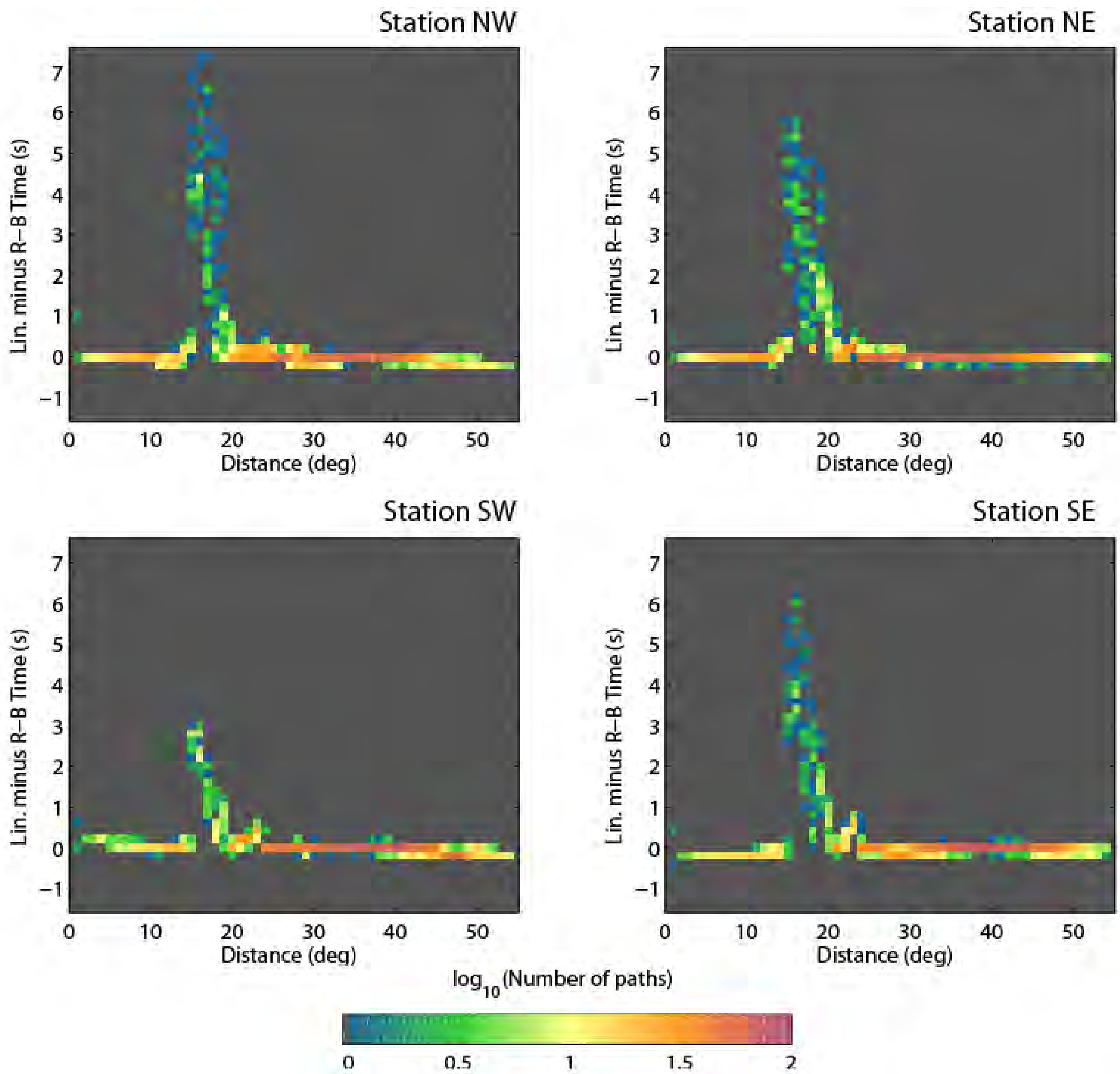

Figure 3. Discrepancy between travel times calculated through model LLNL-G3D with two methods: raybending and linearization with ray warping. Linearized times were calculated with AK135 as the reference model. The discrepancies are displayed as histograms binned by time discrepancy and epicentral distance.

Joint Regional/Teleseismic Tomography

Rodi et al. (2010) showed preliminary results of applying joint regional/teleseismic tomography to update the crust and upper mantle P-wave velocity model for southern Asia developed by Reiter et al. (2009). That model, called JWM, was derived with the joint inversion of regional (predominantly Pn) travel times, which determined the P velocity structure, and Rayleigh-wave group delays, which determined the S velocity structure, applying geostatistical constraints to couple the two data sets. We updated the JWM P-wave model by applying joint tomography to the same Pn data set used to derive JWM combined with teleseismic travel times. Only a single step of an iterative inversion was done, i.e. linearized tomography was performed. The resulting model fit the regional travel-time data as well as JWM while also removing a bias of over one second in the teleseismic times predicted by JWM, thus demonstrating the merits of joint calibration.

We are redoing our joint regional/teleseismic tomography exercise to reflect two enhancements we made to our tomography algorithm. First, we expanded the capacity of the algorithm to handle up to one million travel-time data and one million velocity model parameters (running on a serial processor accessing 16 Gbytes of memory), which allowed us to include data from both teleseismic events and teleseismic stations, together with the regional times, in one inversion. Previously we found it necessary to treat the two types of teleseismic paths separately. The final data set comprises about 140,000 regional arrivals (those used to derive JWM) and 660,000 teleseismic P arrivals covering event-station distances from 25° to 55°.

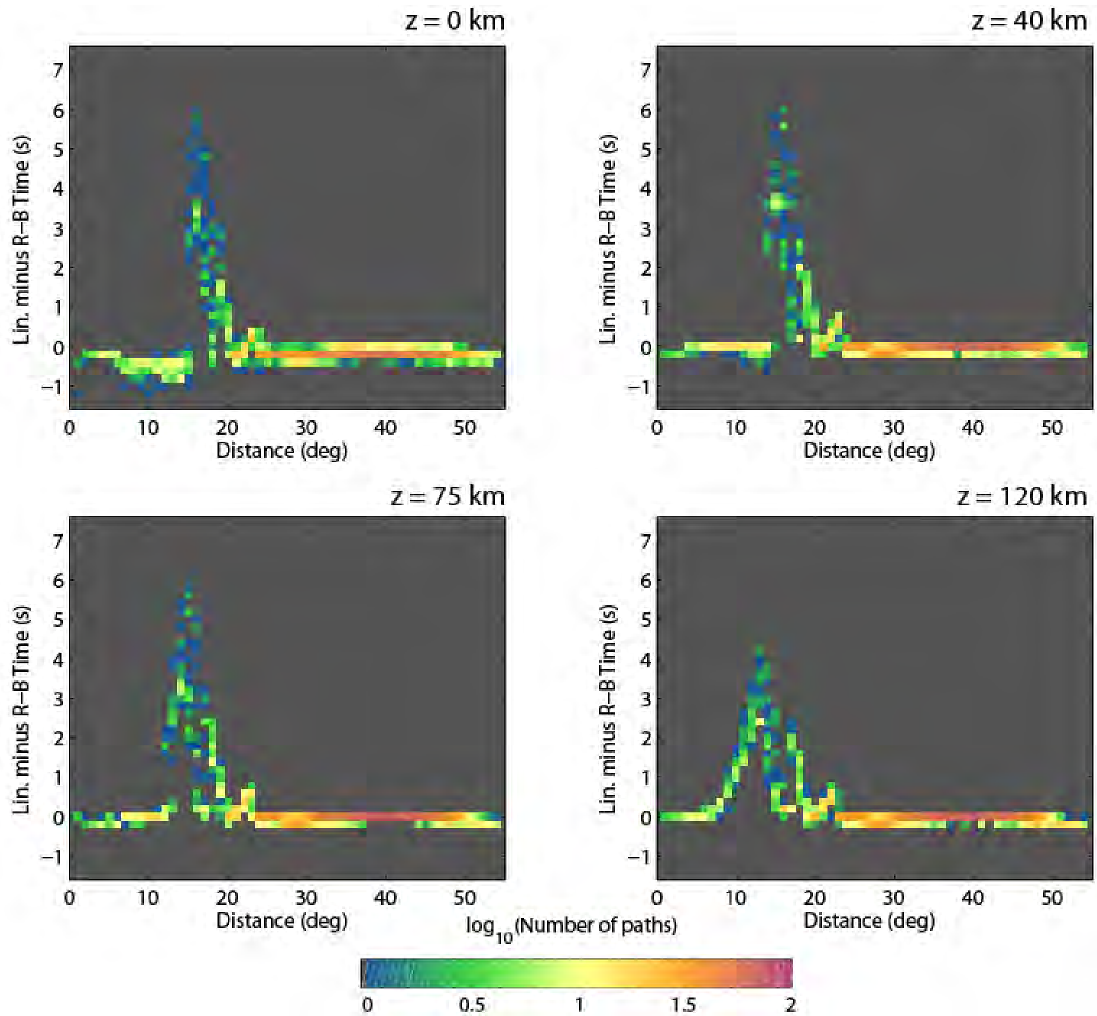

Figure 4. Discrepancy between travel times calculated through model LLNL-G3D with raybending and linearization with ray warping, displayed as histograms binned by time discrepancy and epicentral distance. Linearized times were calculated with AK135 as the reference model. Each panel displays the discrepancies for paths from Station SE to a geographic grid of events at the labeled focal depth, *z*.

The second enhancement we made to our tomography algorithm was the incorporation of our new method for travel-time linearization, based on ray warping, as an optional forward model for regional and teleseismic data. Previously, the algorithm assumed that regional times were linearized (in the standard way) with respect to a 3D model and that teleseismic times were linearized relative to AK135. Normally, the 3D reference model for regional times is the model resulting from the previous iteration of a nonlinear inversion but, in this exercise, it is JWM. We use the Podvin-Lecomte finite difference method (Podvin and Lecomte, 1991) to compute regional travel times in a 3D reference model, and their sensitivities to velocity parameters. Our second enhancement allows regional times to be linearized with respect to AK135, as is done with teleseismic travel times. Additionally, linearization around AK135 can be done with or without ray warping.

As a prelude to generating a new tomographic update of JWM, we tested the accuracy of travel-time linearization, relative to AK135, for modeling the regional data set from southern Asia. The tests compared the linearized times through JWM to Podvin-Lecomte calculations. While the Podvin-Lecomte method is not as accurate as raybending, it is still a full 3D method. Figure 5 shows the result of two tests. In each, linearized times, obtained using AK135 as the reference model, are compared to the Podvin-Lecomte times. The discrepancies shown in the left panel were obtained with the standard linearization method, while those on the right used linearization with ray warping. As in the earlier example with LLNL-G3D, we see that the use of ray warping dramatically reduces the errors in regional travel-time calculations. The errors are somewhat larger than before (c.f. Figure 3), but errors in the Podvin-Lecomte times may be partly to blame.

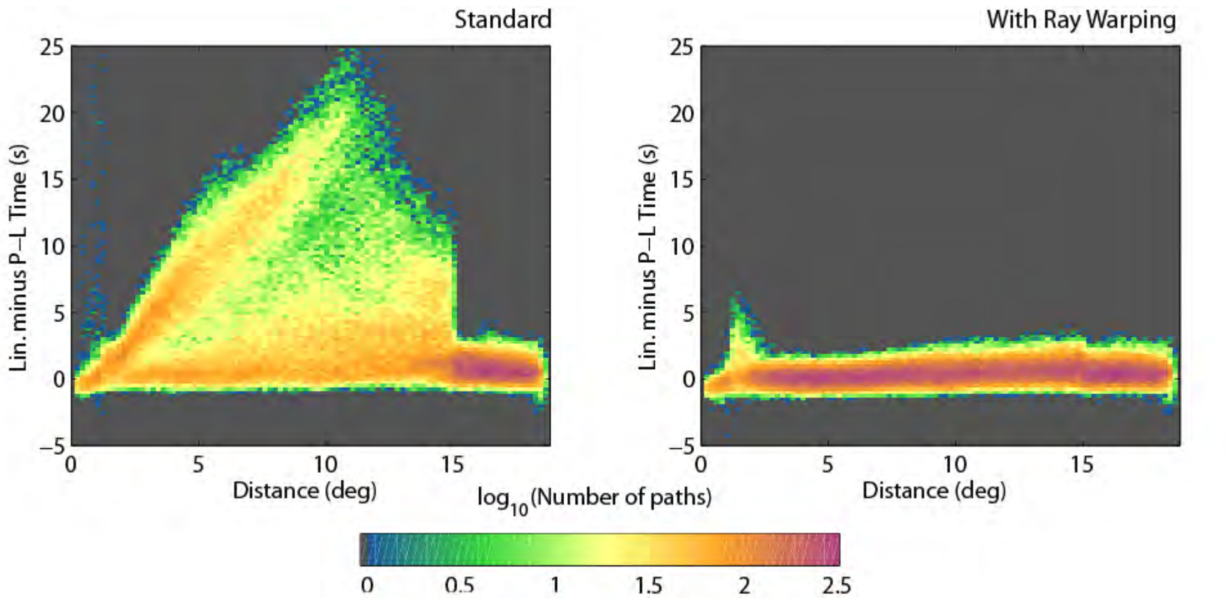

Figure 5. Discrepancy between travel times calculated through model JWM with Podvin-Lecomte raytracing and linearization around AK135. The discrepancies are shown as histograms binned by time and epicentral distance (using bin sizes of 0.1 s and 1°, respectively). *Left:* The standard linearization method was used. *Right:* Linearization with ray warping was used.

Figure 6 shows a vertical slice through models obtained with linearized joint inversion of the regional and teleseismic travel-time data sets from southern Asia. For both models, teleseismic times were linearized with respect to AK135. Ray warping was used, although for teleseismic distances it does not have a big effect. For the inversion model in the top panel, regional times were linearized with respect to the 3D JWM model, as had been done in our previous experiments with joint regional/teleseismic tomography. In this case, Podvin-Lecomte finite-difference raytracing was used to obtain the reference times through JWM and their sensitivities to velocity parameters. For the inversion model in the bottom panel, regional times were linearized with respect to AK135, using the ray warping technique for improved accuracy. We see that the models are very similar to one another, further supporting the adequacy of linearization of regional travel times with respect to a 1D reference model. Further, the main features of both models are similar to those of our earlier joint inversion models (Rodi et al., 2010), which were derived from subsets of the teleseismic data.

CONCLUSIONS AND RECOMMENDATIONS

The numerical techniques we have developed to date have the potential to significantly enhance the practicality of joint regional/teleseismic location and calibration with a unified 3D Earth model. In particular, our modification of travel-time linearization with the use of ray warping seems to extend the applicability of linearization as an efficient alternative to 3D raytracing to regional distances. For which types of 3D structures and which epicentral distances and event depths it can be applied, with acceptable and predictable accuracy, will require further study to determine.

Improving the efficiency of travel-time calculation is important for both event location and travel-time calibration. The task of locating events on a routine basis, using arrival-time picks from a large base of stations changing over time, is greatly simplified if travel times for arbitrary paths can be calculated quickly. Computational efficiency is also crucial in building a unified 3D Earth model via tomographic inversion of large travel-time data sets. Among other reasons, it facilitates the challenging task of computing model uncertainty. Beyond computational speed, the validity of a linear approximation to travel times is valuable in and of itself, allowing iterative inversion schemes to converge faster and increasing the validity of uncertainty measures that are based on linear inverse theory.

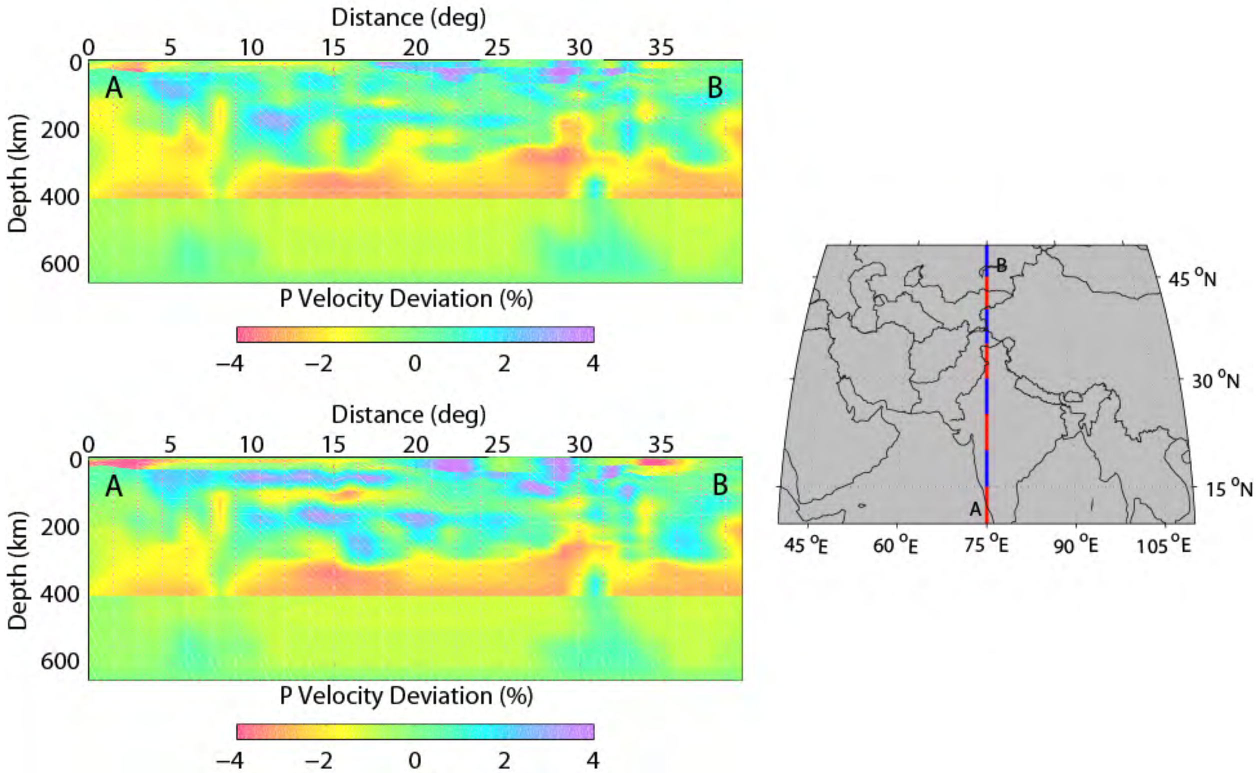

Figure 6. A vertical slice (Line A-B in map to the right) through two 3D P velocity models obtained with linearized joint inversion of regional and teleseismic P-wave travel times. Each is shown in terms of its velocity deviation from model JWM. The inversion models are both based on linearization of teleseismic travel times relative to the AK135 model, but used different modeling technique for regional (Pn) times. *Top*: Regional travel times are linearized with respect to JWM, with reference travel times and their sensitivities computed with the Podvin-Lecomte method. *Bottom*: Regional times are linearized relative to AK135, using 1D raytracing with ray warping to compute reference times and sensitivities.

REFERENCES

Antolik, M., Y. J. Gu, G. Ekström, and A. M. Dziewonski (2003). J362D28: a new joint model of compressional and shear velocity in the Earth's mantle, *Geophys. J. Int* 153:2, 443–466.

Engdahl E. R., R. van der Hilst, and R. Buland (1998). Global teleseismic earthquake relocation with improved travel times and procedures for depth determination, *Bull. Seismol. Soc. Am*. 88: 722–743.

Flanagan, M. P., S. C. Myers, and K. D. Koper (2007). Regional travel-time uncertainty and seismic location improvement using a three-dimensional a priori velocity model, *Bull. Seismol. Soc. Am*. 97: 804–825.

Kennett, B. L. N., E. R. Engdahl, and R. Buland (1995). Constraints on the velocity structure in the Earth from travel times, *Geophys. J. Int*. 122: 108–124.

Murphy, J. R., W. Rodi, M. Johnson, D. D. Sultanov, T. J. Bennett, M. N. Toksöz, V. Ovtchinnikov, B.W. Barker, D.T. Reiter, A.C. Rosca, and Y. Shchukin (2005). Calibration of International Monitoring System (IMS) stations in central and eastern Asia for improved seismic event location, *Bull. Seismol. Soc. Am*. 95: 1535–1560.

Myers, S. C., G. Johannesson, and N. A. Simmons (2011). Global-scale P wave tomography optimized for prediction of teleseismic and regional travel times for Middle East events: 1. Data set development, *J. Geophys. Res*. 116: B04304, doi:10.1029/2010JB007967.

Podvin, P., and I. Lecomte (1991). Finite difference computation of traveltimes in very contrasted velocity models: a massively parallel approach and its associated tools, *Geophys. J. Int.* 105: 271–284.

Rawlinson, N.. and M. Sambridge (2004). Wave front evolution in strongly heterogeneous layered media using the fast marching method, *Geophys. J. Int*. 156: 631–647.

Reiter, D. T., and W. L. Rodi (2009). Validated 3D velocity models in Asia from joint regional body- and surface-wave tomography. Final Report, *Weston Geophysical Corp.*, AFRL-RV-HA-TR-2009-1009.

Reiter, D., W. Rodi, and M. Johnson (2005). Development of a tomographic upper mantle velocity model beneath Pakistan and northern India for improved regional seismic event location, *Bull. Seismol. Soc. Am*. 95: 926–940.

Ritzwoller, M. H., N. M. Shapiro, M. P. Barmin, and A. L. Levshin (2002). Global surface wave diffraction tomography, *J. Geophys. Res*. 107: doi: 10.1029/2002JB001777.

Rodi, W. L., D. T. Reiter, S. C. Myers, and N. A. Simmons (2010). A unified approach to joint regional/teleseismic calibration and event location with a 3D Earth model, *Proceedings of the 2010 Monitoring Research Review: Ground-Based Nuclear Explosion Monitoring Technologies,* LA-UR-10-05578, Vol. 1, pp. 338–347.

Ryaboy, V., D. R. Baumgardt, P. Firbas, and A. M. Dainty (2001). Application of 3-D crustal and upper mantle velocity model of North America for location of regional seismic events, *Pure Appl. Geophys*. 158: 79–103.

Simmons, N. A., S. C. Myers, and A. Ramirez (2009). Multi-resolution seismic tomography based on recursive tessellation hierarchy, in *Proceedings of the 2009 Monitoring Research Review*: *Ground-Based Nuclear Explosion Monitoring Technologies*, LA-UR-09-05276, Vol. 1, pp. 211–220.

Simmons, N. A., S. C. Myers, and G. Johannesson (2011). Global-scale P wave tomography optimized for prediction of teleseismic and regional travel times for Middle East events: 2. Tomographic inversion, *J. Geophys. Res*. 116: B04305, doi:10.1029/2010JB007969.

Um, J. and C. H. Thurber (1987). A fast algorithm for two-point seismic ray tracing, *Bull. Seismol. Soc. Am.* 77: 972–986.

Yang, X. P., I. Bondar, J. Bhattacharyya, N. Shapiro, M. Antolik, G. Ekstrom, H. Israelsson, and K. McLaughlin (2004). Validation of regional and teleseismic travel-time models by relocating ground-truth events, *Bull. Seismol. Soc. Am*. 94: 897–919.